(Received 12 February 2026, Accepted 10 April 2026, Scheduled 24 April 2026)

High-Performance Double-Sided Axe-Shaped Antenna Based on DGS with Multi-Band for WiMAX/WLAN/X-Band Applications

Yousif M. Hasan* and Hassan H. Naji

Department of Electronic and Communication Engineering, College of Engineering, University of Al-Qadisiyah, Iraq

ABSTRACT: This study presents a novel double-sided axe-shaped antenna with a triple band for multi-band applications. The presented antenna features a circular ring and two ring sectors as a double-sided axe-shaped patch antenna to generate three resonant frequencies, WiMAX 3.55 GHz (3.5–3.62 GHz), WLAN 5.12 GHz (5–5.28 GHz), and X-band 7.67 GHz (7.18–8.17 GHz), with reflection coefficients of -14.86 dB, -19.36 dB, and -36.96 dB, respectively. The proposed antenna is fabricated on an FR4 ($\epsilon_r = 4.3$) substrate with dimensions of $30 \times 30 \times 1.6\,\text{mm}^3$ and uses DGS ground to improve the current distribution and impedance bandwidth. The proposed antenna is successfully simulated and measured. The performance evaluation of the multi-band antenna demonstrated satisfactory agreement between simulations and measurements. The proposed multi-band antenna combines enhanced performance with a compact size.

1. INTRODUCTION

With the fast growth of wireless communication systems, multi-band antennas of high efficiency and good realized gain have become critical for numerous applications, including WLAN, WiMAX, Wi-Fi, GPS, and other wireless applications [1]. The need to design multi-band antennas capable of meeting the requirements of these diverse applications is becoming increasingly important. Many researchers have designed antennas for single-band, ultra-wideband (UWB), and multi-band wireless communications. Despite significant progress in antenna design, challenges remain related to achieving reduced physical size, high gain, and efficiently covering multiple frequency bands. Furthermore, most current designs focus on a single frequency band, limiting their flexibility in adapting to different applications. Several studies have indicated that the antenna design in the internet of things (IoT) systems must balance several factors, including size, efficiency, and bandwidth [2]. A single-band antenna with a size of $55 \times 60\,\text{mm}^2$ is presented in [3] for covering the ultra-high frequency (UHF) band with a frequency range of 892–940 MHz and achieving a gain value of 1.76 dBi. UWB antennas are presented in [4, 5], which cover UWB with a dual-band notch for the underlay CR applications. In study [6], a UWB antenna is proposed for 5G IoT applications with a range of realized gain from 3 to 8 dBi with a whole size of $116 \times 93\,\text{mm}^2$. A simple rectangular antenna operating at a frequency of 361 MHz with a realized gain of 1.142 dBi is proposed in [7] for IoT applications. A rectangular slotted patch antenna is presented in the study for UWB applications with a compact size of $22 \times 35\,\text{mm}^2$ and a realized gain value of 4.8 dBi [8]. Efficient methods have been proposed by many researchers for creating multi-band antennas, such as dual-band antennas [9–17], triple-band antennas [18–22], and quad-band antennas [23–25]. A dual-band antenna operating in mid-band 5G and LTE-40 using a concentric circular ring structure with a size of $32 \times 24 \times 1.6\,\text{mm}^3$ is presented in [15]. A dual-band antenna with a coplanar waveguide (CPW) intended for WLAN and WiMAX networks composed of an inverted L-shaped slot resonator, which is coupled with a U-shaped ground plane, was introduced in [16]. A filtenna system with three modes for UWB, WiMAX, and WLAN with realized gains of 2.2 dBi, 2.65 dBi, and 1.92 dBi, respectively, is presented in [19] for cognitive radio (CR) applications. In study [22], a triband antenna with a size of $33 \times 22\,\text{mm}^2$ based on split-square and half-ring resonators was proposed to operate at frequencies of 2.4, 3.7, and 5.8 GHz with gains of 1.43 dBi, 0.89 dBi, and 1 dBi for IoT applications. In study [26], a monopole antenna featuring three concentric semicircular rings was presented to generate a triband for GSM, 4G LTE, and 5G applications. Most of the previous works on circular ring antennas for multi-band applications show that the size of the antenna is quite large and has low realized gain. Therefore, this study aims to present an innovative design for a low-cost, compact antenna that operates in three frequency bands and has high gain, making it suitable for IoT applications. This study presents a microstrip antenna design based on a novel double-sided axe-shaped radiating element and features multi-band operation. The proposed antenna features three main frequency bands for multi-band applications: the lower band covers the frequency range from 3.5 to 3.62 GHz, making it appropriate for wireless communication applications, such as 5G and WiMAX bands.

The second band covers 5 to 5.28 GHz with a -10 dB bandwidth, making it appropriate for the WLAN band. The upper band covers the 7.18–8.17 GHz range and is part of the UWB, making it suitable for X-band radar applications. The peak gains achieved by the proposed antenna are 3.6 dBi, 3.95 dBi, and 4 dBi at the three resonant frequencies, respectively. The

* Corresponding author: Yousif Mohsin Hasan (yousif.hasan@qu.edu.iq).

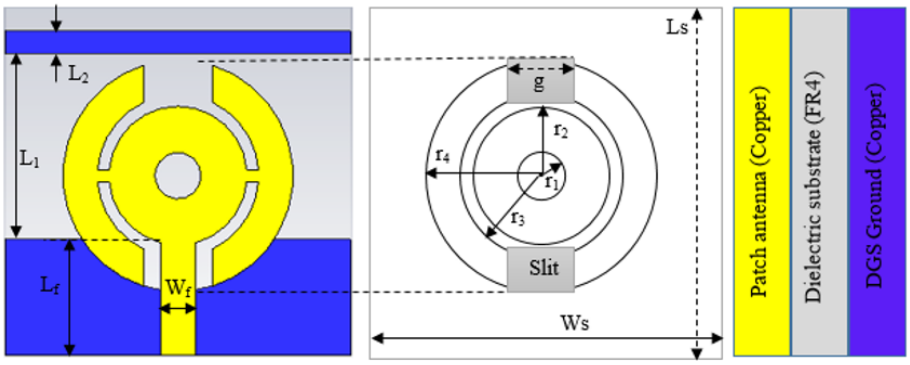

FIGURE 1. The layout and geometry of the proposed double-sided axe-shaped antenna.

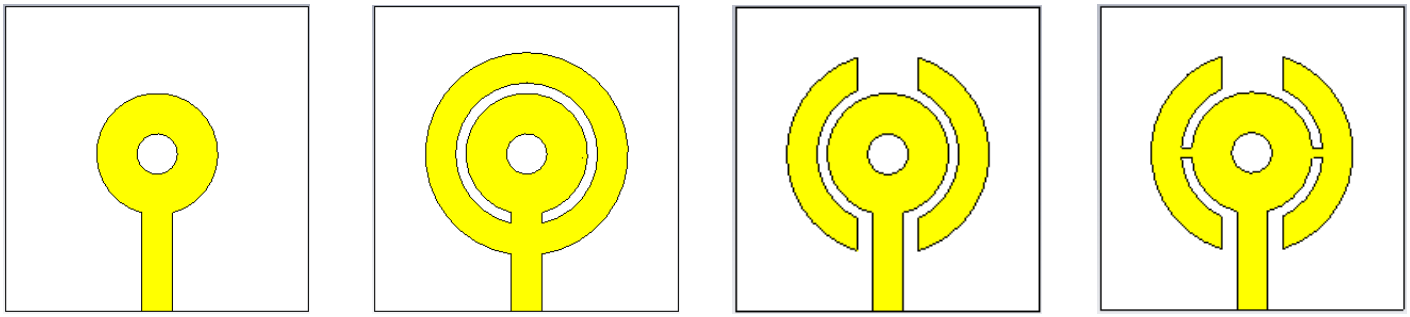

(Ant1) (Ant2) (Ant3) (Ant4)

FIGURE 2. Four steps to design and optimize the proposed double-sided axe-shaped antenna.

narrowband of the tri-band resonant frequencies intended for 5G, WiMAX, WLLAN, and X-band makes the proposed antenna suitable for IoT applications. This paper is divided into the following sections. Section 2 describes the double-sided axe-shaped antenna design. Section 3 includes the parametric study of the proposed antenna. Section 4 exhibits the results of the proposed antenna and compares them to other multi-band works. The conclusion is provided in Section 5.

2. DOUBLE-SIDED AXE-SHAPED ANTENNA DESIGN

Figure 1 shows the geometric design of the proposed antenna, a double-sided axe-shaped patch antenna, which was modeled, optimized, and simulated using Computer Simulation Technology (CST) Microwave Studio. Two identical ring-sector-shaped resonators were placed on either side of a concentric circular ring. The circular ring was directly connected to the feed line, and the two ring-sector-shaped resonators were fed through two parasitic elements connected to the inner ring to create a double-sided, axe-shaped structure. The proposed antenna was designed and optimized in four steps. The initial antenna used a conventional circular-ring resonator, which is fed directly from the transmission feedline as shown in Figure 2 (Ant1), and in this step, the reflection coefficient is impedance-mismatching and has no resonant frequency, so it shows S_{11} above -10 dB. In the next step, another circular ring was inserted as an outer ring resonator, as in Figure 2 (Ant2), to generate the single band at the resonant frequency of 7.38 GHz. Figure 2 (Ant3) shows the outer ring transformed into two identical ring sectors by cutting two slits of width g opposite to each other to provide dual bands at 4.98 and 6.74 GHz. In the final step, two small parasitic elements are connected between the inner ring and the two ring sectors, as shown in Figure 2 (Ant4), with tri-bands with resonant frequencies at 3.5, 5.06, and 7.74 GHz. The proposed antenna has compact dimensions of 30 mm $\times$ 30 mm, and the main parameter values are listed in Table 1.

Figure 3 shows the reflection coefficient (S_{11}) for the four steps to optimize and design the proposed double-sided axe-shaped antenna. The reflection coefficient of the proposed antenna (Ant4) shows that it operates at three resonant frequencies. All resonant frequencies of the four-step design of the antenna are listed in Table 2.

3. PARAMETRIC STUDY OF THE PROPOSED ANTENNA

In this section, we discuss the effect of two slits with width g and the defected ground structure on the performance of the proposed multi-band antenna. Figure 4 shows the effect of a gap g on the S-parameter (S_{11}) of the antenna. The parametric study shows that when increasing the gap g from 3 to 8 mm with a step of 1 mm, the optimized tri-band reflection coefficient is at the value of 6 mm. Varying the gap value from 0 to 3 mm does not affect the reflection coefficient of the antenna. The second one is the effect of changing the radius of the ring sector r_3 shown in Figure 5. It is noticeable that when r_3 is increased,

TABLE 1. Parameter values in mm of the single antenna element.

Parameter	W_s	L_s	W_f	L_f	L_1	L_2	g	r_1	r_2	r_3	r_4
Values	30	30	3	10	16	2	6	2	6	7	10

TABLE 2. Resonant frequencies of the four-step design to develop proposed antenna.

Steps	Ant1	Ant2	Ant3	Ant4
Resonant frequencies in GHz	S_{11} Above -10 dB	7.38	4.98 and 6.74	3.5, 5.06, and 7.74

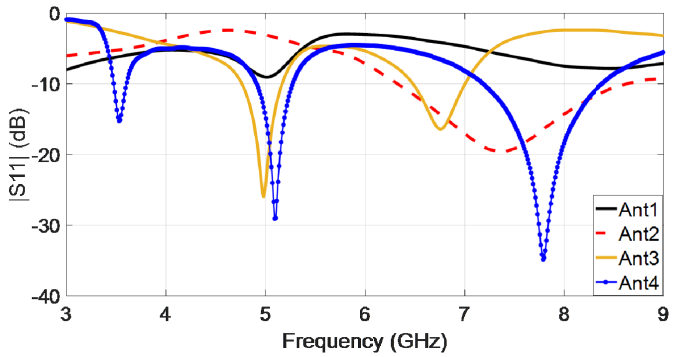

FIGURE 3. The reflection coefficients of four steps to design and optimize the proposed antenna.

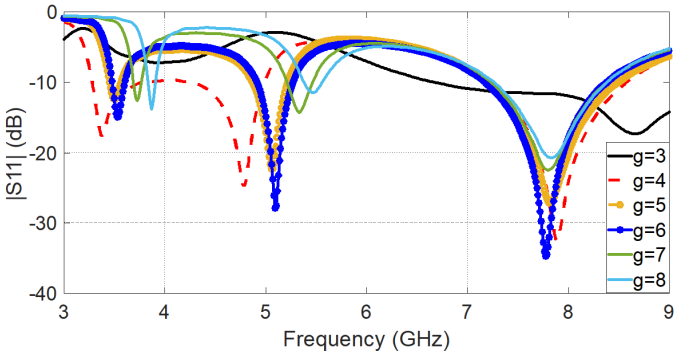

FIGURE 4. The effect of inserting two slits with width g on the S_{11} of the proposed antenna.

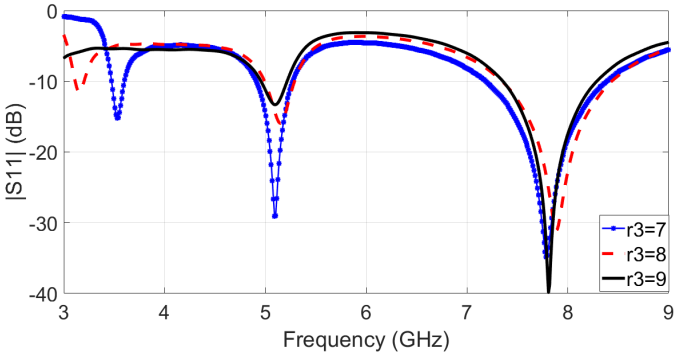

FIGURE 5. The effect of increasing the radius of the ring sector on the reflection coefficient of the proposed antenna.

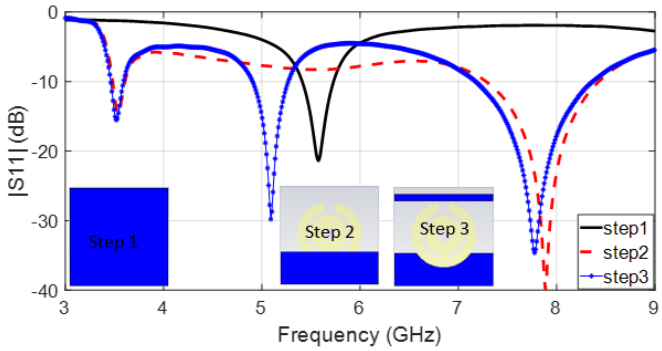

FIGURE 6. The reflection coefficients of three steps of the ground plan of the proposed antenna.

the first lower frequency decreases, and its reflection coefficient value increases above -10 dB, while the other two bands are not affected so much.

The third parametric study is considered when using a defected ground structure (DGS) to improve the performance parameters of the proposed tri-band antenna. Figure 6 shows the effect of DGS on the S_{11} of the proposed antenna for the three steps. A full ground plane is used in step 1; however, in this case, the reflection coefficient shows a single resonant frequency at 5.6 GHz. In step 2, partial ground structure, the reflection coefficient shows that the antenna operates at two frequencies, 3.529 GHz and 7.889 GHz. In step 3, a defected ground structure is used; an inverted semicircle is etched from the partial ground, and a parasitic element has also been added above to enhance the antenna's parameters. In this step, the antenna operates tri-bands with resonant frequencies of 3.5, 5.06, and 7.74 GHz. Good impedance matching is achieved when using DGS compared to full ground and standard partial ground.

4. SIMULATION AND MEASUREMENT RESULTS

Figure 7 shows the front and back prototypes of the proposed antenna, which is printed on an FR4 substrate. Reflection coefficient of the proposed antenna was measured using Vector Network Analyzer (Anritsu MS4642A-20 GHz) package.

4.1. Reflection Coefficient (S_{11})

The simulated (measured) value of the s-parameter of the proposed double-sided axe-shaped antenna is shown in

TABLE 3. The simulated and measured results of the proposed tri-band antenna.

Band	Results	Operating frequency (GHz)	Impedance bandwidth (GHz)	S_{11} (dB)	Realized gain (dBi)	Radiation efficiency (%)
Band 1	Sim.	3.5	3.44–3.59	−15	4	95
	Meas.	3.55	3.5–3.62	−14.86	3.6	93
Band 2	Sim.	5.06	4.87–5.24	−27.9	5.28	72
	Meas.	5.12	5–5.28	−19.36	3.95	80
Band 3	Sim.	7.74	7.12–8.36	−34.74	4.2	76
	Meas.	7.67	7.18–8.17	−36.96	4	82

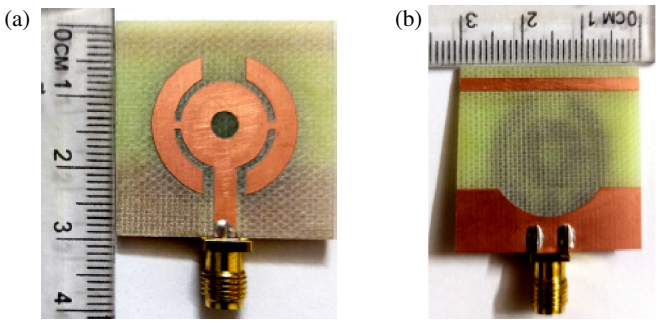

FIGURE 7. The prototype of the proposed double-sided axe-shaped antenna, (a) the front side and (b) the back side.

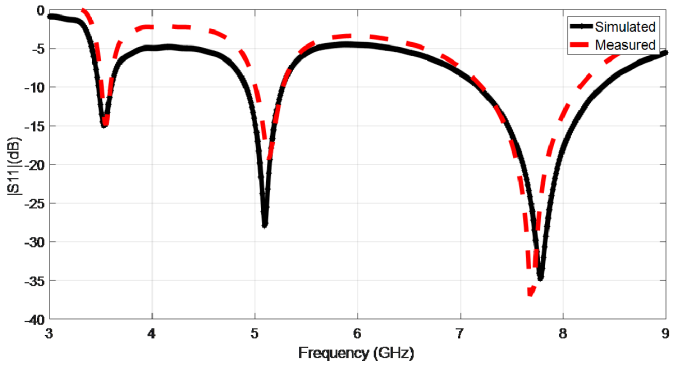

FIGURE 8. The s-parameter (S_{11}) of the proposed antenna.

Figure 8. The results indicate that the proposed antenna operated at tri-bands, with the lower band at a frequency of 3.5 GHz (3.55 GHz) and a covering frequency bandwidth of 3.44–3.59 GHz (3.5–3.62 GHz) with an S-parameter (S_{11}) value of −15 dB (−14.86 dB). The bandwidth of the second band is 4.87–5.24 GHz (5–5.28 GHz) with a center frequency of 5.06 GHz (5.12 GHz) and an S_{11} of −27.9 dB (−19.36 dB). The upper band is 7.12–8.36 GHz (7.18–8.17) with a reflection coefficient of −34.74 dB (−36.96 dB) at the operating frequency of 7.74 GHz (7.67 GHz). The results show that the proposed antenna is suitable and covers 5G, WiMAX, WLAN, and X-band for IoT applications.

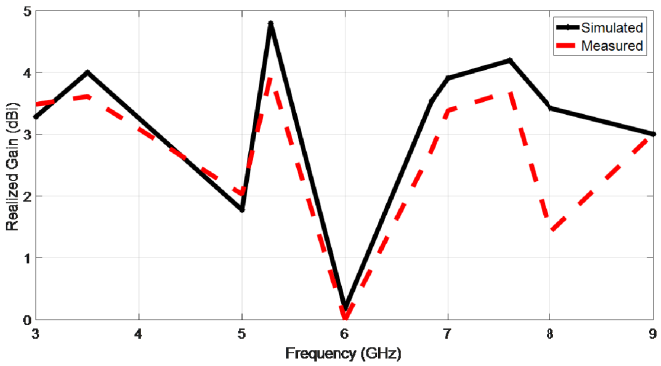

FIGURE 9. The realized gain (dBi) of the proposed antenna.

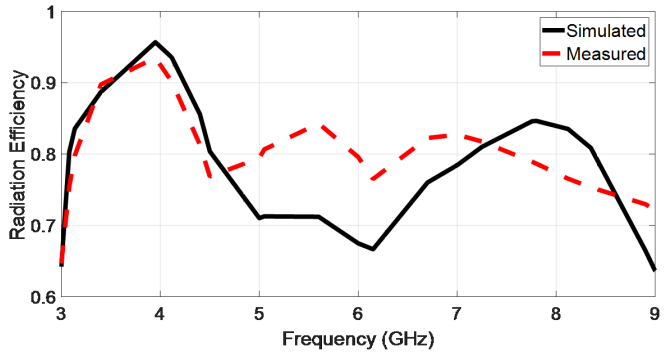

FIGURE 10. The radiation efficiency of the proposed antenna.

4.2. Radiation Efficiency and Realized Gain

Figure 9 shows the simulated (measured) realized gain of the proposed antenna at three resonant frequencies, with peak realized gains of 4 dBi (3.6 dBi), 5.28 dBi (3.95 dBi), and 4.2 dBi (4 dBi). The radiation efficiency values of the proposed antenna are illustrated in Figure 10, which shows that at all resonance frequencies, the radiation efficiency levels are higher than 72%. Table 3 summarizes all the simulated and measured results for the proposed tri-band antenna. The modest disparity between the measured and simulated findings might be attributed to probable manufacturing faults, as well as the manner in which the measurements were obtained using a network analyzer.

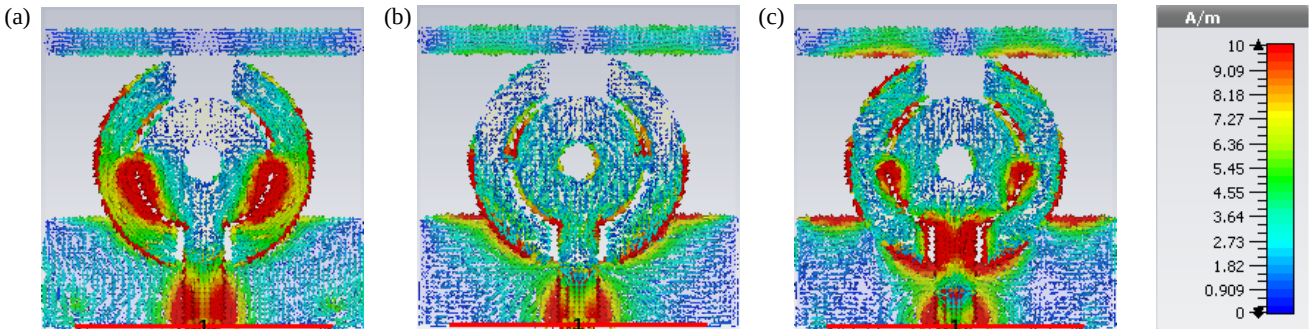

FIGURE 11. Simulated current surface distribution of the proposed multi-band antenna at resonant frequencies (a) 3.5 GHz, (b) 5.06 GHz, and (c) 7.74 GHz.

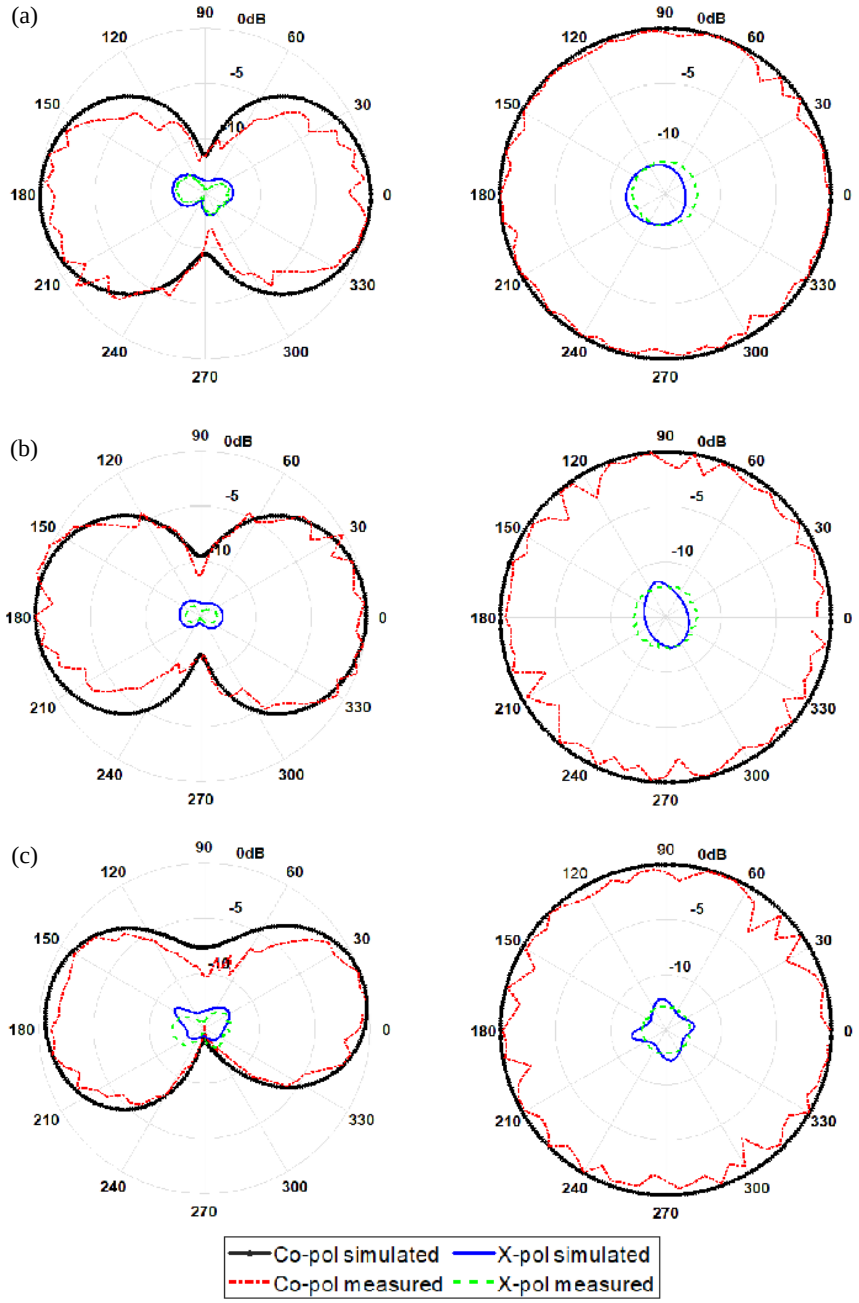

FIGURE 12. Power pattern E-plane (x-z plane) on the left and H-plane (y-z plane) on the right of the antenna at three operating frequencies at (a) 3.5 GHz, (b) 5.06 GHz, and (c) 7.74 GHz.

TABLE 4. Performance comparison of the proposed antenna with other multi-band works.

Ref. No.	Size (mm^2)	Substrate	frequencies (GHz)	Bandwidth (GHz)	Gain (dBi)
[22]	33×22	FR4	2.4, 3.7, 5.8	0.3, 0.39, 0.9	1.43, 0.9, 1.1
[27]	17×33	FR4	3.1, 2.4, 6	2.2, 1, 2	1, 1.6, 2.2
[28]	16×25	NA	2.3, 3.3, 6.5	1, 0.7, 1.9	1.4, 2, 4.1
[29]	86×61	FR4	2.6, 3.8, 5.3	1.1, 1.2, 0.6	2.9, 2.5, 3.8
[30]	26×25	RO4350	2.45, 3.5, 5.8	0.39, 0.39, 0.76	6.3, 7.4, 8.7
[31]	80×80	FR4	2.46, 3.59, 5.69	0.14	2.33, 3.14, 2.89
This work	30×30	FR4	3.55, 5.12, 7.67	0.12, 0.28, 0.99	3.6, 3.95, 4

4.3. Surface Current Distribution

Figures 11(a)–(c) highlight the surface current distribution of the proposed antenna at three simulated resonant frequencies of 3.5, 5.06, and 7.74 GHz, respectively. The results showed a distinct surface current distribution at the tri-bands with three resonant frequencies. In the lower band at 3.5 GHz, the current is observed to be intensely concentrated in the active regions of the antenna, specifically the region between the two rings of the radiating patch element and feed lines. In the second band at 5.06 GHz, the current is distributed on the outer ring circumference. In contrast, in the upper band, the current distribution shifts and concentrates at the lower end radiating element at a frequency of 7.74 GHz, reflecting the efficient structure design of the proposed antenna and the optimal resonance mechanism in the upper band.

4.4. Power Pattern of the Proposed Antenna

Figure 12 shows the co-polarization and cross-polarization in the E-plane (left) and H-plane (right) power patterns of the proposed antenna at the three operating frequencies of 3.5, 5.06, and 7.74 GHz. The radiation patterns of the antenna were calibrated based on the realized gain at the three operating frequencies. The omnidirectional and bidirectional characteristics in the H-plane (yz-plane) and E-plane (xz-plane), respectively, demonstrate that this antenna can radiate in all directions, making it suitable for use with multi-band devices. The cross-polarization level of the proposed antenna remains lower than -15 dB at all three resonant frequencies. Table 4 compares the proposed multi-band antenna with those in the literature. The comparison revealed that the proposed antenna is superior to other works in terms of small size, low cost, high realized gain values, and good radiation efficiency.

5. CONCLUSIONS

This study presents a novel compact antenna based on a double-sided, axe-shaped radiating element, featuring multi-band operation. The proposed tri-band antenna has been successfully simulated and fabricated. Two ring sector resonators were used to generate three resonant frequencies. The patch antenna is fabricated on the top layer, while the DGS partial ground enhances the performance of the proposed multi-band antenna. The proposed design has high performance, such as an adequate 4 dBi gain and approximately 80% radiation efficiency. The proposed antenna features three main frequency bands: the lower band covers the frequency range from 3.5 to 3.62 GHz with a -10 dB bandwidth, making it appropriate for wireless communication applications, such as 5G and WiMAX. The second band covers frequencies 5–5.28 GHz, including WLAN. The upper band extends from 7.18 to 8.17 GHz and is part of the UWB, making it appropriate for X-band radar applications. For future works, it is recommended to redesign the proposed antenna using another substrate material with a tangent loss lower than FR4. Furthermore, the proposed antenna can be modified to a reconfigurable antenna for future communications. A PIN or varactor diode could be attached within the gap g of the ring sector to achieve discrete or continuous tunable bands.

REFERENCES

[1] Hasan, Y. M., Z.-A. Rahman, and Y. Al-Yasir, "A miniature hexa-band antenna for internet of things applications using six quarter-wavelength resonators," *Advanced Electromagnetics*, Vol. 14, No. 1, 52–58, 2025.

[2] Al-Fuqaha, A., M. Guizani, M. Mohammadi, M. Aledhari, and M. Ayyash, "Internet of things: A survey on enabling technologies, protocols, and applications," *IEEE Communications Surveys & Tutorials*, Vol. 17, No. 4, 2347–2376, 2015.

[3] Abdulzahra, D. H., F. M. Alnahwi, and A. S. Abdullah, "A highly compact and low cost UHF wide slot antenna for internet of a things applications," *Journal of Electrical Engineering & Technology*, Vol. 19, No. 4, 2501–2509, 2024.

[4] Hasan, Y. M., A. S. Abdullah, and F. M. Alnahwi, "UWB filtenna with reconfigurable and sharp dual-band notches for underlay cognitive radio applications," *Progress In Electromagnetics Research C*, Vol. 120, 45–60, 2022.

[5] Hasan, Y. M., K. D. Rahi, and A. A. Mahmood, "Rectangular antenna with dual-notch band characteristics for UWB applications," in *AIP Conference Proceedings*, Vol. 2591, No. 1, 020032, 2023.

[6] Rao, I. R. K., R. S. Nayak, and K. Rajasekhar, "Design and performance evaluation of a single-layer planar UWB antenna for omnidirectional coverage of 5G IoT devices," *Progress In Electromagnetics Research C*, Vol. 157, 101–107, 2025.

[7] Abdulzahra, D. H., F. M. Alnahwi, and A. S. Abdullah, "Design of a miniaturized printed antenna for 2.4 GHz IoT applications," *International Journal on Communications Antenna and Propagation (IRECAP)*, Vol. 12, No. 3, 198–205, 2022.

[8] Hasan, Y. M., "A compact monopole slotted patch-antenna for UWB applications," *Progress In Electromagnetics Research C*, Vol. 151, 65–71, 2025.

[9] Abdulkawi, W. M., A. F. A. Sheta, I. Elshafiey, and M. A. Alkanhal, "Design of low-profile single-and dual-band antennas for IoT applications," *Electronics*, Vol. 10, No. 22, 2766, 2021.

[10] Hasan, Y. M., A. S. Abdullah, and F. M. Alnahwi, "Dual-port filtenna system for interweave cognitive radio applications," *Iranian Journal of Science and Technology, Transactions of Electrical Engineering*, Vol. 46, No. 4, 943–958, 2022.

[11] Fazal, D. and Q. U. Khan, "Dual-band dual-polarized patch antenna using characteristic mode analysis," *IEEE Transactions on Antennas and Propagation*, Vol. 70, No. 3, 2271–2276, 2022.

[12] Muzaffar, S., D. Turab, M. Zahid, and Y. Amin, "Dual-band UWB monopole antenna for IoT applications," *Engineering Proceedings*, Vol. 46, No. 1, 29, 2023.

[13] Pradeep, P., J. S. Kottareddygari, and C. S. Paidimarry, "Design of a dual-band monopole antenna for Internet of Things and sub-6 GHz 5G applications," in *2024 IEEE Wireless Antenna and Microwave Symposium (WAMS)*, 1–4, Visakhapatnam, India, 2024.

[14] Ketavath, K. N., "Dual-band crescent-shaped slot patch antenna for wireless communications and IoT applications," *Microwave and Optical Technology Letters*, Vol. 65, No. 8, 2392–2398, 2023.

[15] Gunamony, S. L. and J. B. Gnanadhas, "Design and investigations of miniaturized dual-band quarter concentric circular ring antenna for LTE and 5G applications," *Arabian Journal for Science and Engineering*, Vol. 46, No. 10, 9617–9626, 2021.

[16] Yadav, A. K., S. Lata, S. K. Singh, A. K. Singh, T. Sharan, and M. Z. A. Yahya, "Investigating the $|S_{11}|$ parameter of CPW-fed antennas for WiMAX and WLAN applications," *Journal of Electronic Materials*, Vol. 52, No. 7, 4359–4368, 2023.

[17] Najumunnisa, M., A. S. C. Sastry, B. T. P. Madhav, S. Das, N. Hussain, S. S. Ali, and M. Aslam, "A metamaterial inspired AMC backed dual band antenna for ISM and RFID applications," *Sensors*, Vol. 22, No. 20, 8065, 2022.

[18] Ahmad, S., H. Boubakar, S. Naseer, M. E. Alim, Y. A. Sheikh, A. Ghaffar, A. J. A. Al-Gburi, and N. O. Parchin, "Design of a tri-band wearable antenna for millimeter-wave 5G applications," *Sensors*, Vol. 22, No. 20, 8012, 2022.

[19] Hasan, Y., A. Abdullah, and F. Alnahwi, "Three-modes, reconfigurable filtenna system with UWB, WiMAX, and WLAN states for cognitive radio applications," *International Journal on Communications Antenna and Propagation (IRECAP)*, Vol. 14, No. 1, 15–23, 2024.

[20] Sharma, S. K., T. Khan, and A. P. Singh, "Tri-band antenna with metasurface-based ground plane for Sub-6 GHz 5G and 6G WPT applications," *Journal of Electromagnetic Waves and Applications*, Vol. 38, No. 10, 1147–1157, 2024.

[21] Alaoui, N., B. A. Amel, and Z. Aya, "Tri-band frequency reconfigurable antenna for wireless applications," *Instrumentation, Mesures, Métrologies*, Vol. 23, No. 2, 175, 2024.

[22] Abdulzahra, D. H., F. Alnahwi, A. S. Abdullah, Y. I. A. Al-Yasir, and R. A. Abd-Alhameed, "A miniaturized triple-band antenna based on square split ring for IoT applications," *Electronics*, Vol. 11, No. 18, 2818, 2022.

[23] Kumar, A. and A. P. S. Pharwaha, "Development of a modified hilbert curve fractal antenna for multiband applications," *IETE Journal of Research*, Vol. 68, No. 5, 3597–3606, 2022.

[24] Ali, W., N. Nizam-Uddin, W. M. Abdulkawi, A. Masood, A. Hassan, J. A. Nasir, and M. A. Khan, "Design and analysis of a quad-band antenna for IoT and wearable RFID applications," *Electronics*, Vol. 13, No. 4, 700, 2024.

[25] Thiruvenkadam, S. and E. Parthasarathy, "Compact multiband monopole antenna design for IoT applications," *Journal of Electromagnetic Waves and Applications*, Vol. 37, No. 5, 629–643, 2023.

[26] Let, G. S., G. J. Bala, C. B. Pratap, D. K. Janapala, and T. Kezia, "Concentric semi-circular ring loaded multi-band antenna for wireless applications," *Analog Integrated Circuits and Signal Processing*, Vol. 114, No. 1, 113–124, 2023.

[27] Karthikeyan, M., R. Sitharthan, T. Ali, and B. Roy, "Compact multiband CPW fed monopole antenna with square ring and T-shaped strips," *Microwave and Optical Technology Letters*, Vol. 62, No. 2, 926–932, 2020.

[28] Jha, P., A. Kumar, A. De, and R. K. Jain, "CPW-fed metamaterial inspired compact multiband antenna for LTE/5G/WLAN communication," *Frequenz*, Vol. 76, No. 7–8, 401–407, 2022.

[29] Wang, L., J. Yu, T. Xie, and K. Bi, "A novel multiband fractal antenna for wireless application," *International Journal of Antennas and Propagation*, Vol. 2021, No. 1, 9926753, 2021.

[30] Li, R., C. Wu, X. Sun, Y. Zhao, and W. Luo, "An EBG-based triple-band wearable antenna for WBAN applications," *Micromachines*, Vol. 13, No. 11, 1938, 2022.

[31] Saghati, A. P., M. Azarmanesh, and R. Zaker, "A novel switchable single-and multifrequency triple-slot antenna for 2.4-GHz bluetooth, 3.5-GHz WiMax, and 5.8-GHz WLAN," *IEEE Antennas and Wireless Propagation Letters*, Vol. 9, 534–537, 2010.